

Received May 31, 2020, accepted June 28, 2020, date of publication July 8, 2020, date of current version July 21, 2020.

Digital Object Identifier 10.1109/ACCESS.2020.3006964

# Tracking Control of PZT-Driven Compliant Precision Positioning Micromanipulator

ZHIGANG WU<sup>1</sup>, MIN CHEN<sup>1</sup>, PING HE<sup>2</sup>, HENG LI<sup>3</sup>, QI ZHANG<sup>4</sup>, (Member, IEEE),  
XINGZHONG XIONG<sup>5</sup>, HAO-YANG MI<sup>6</sup>, ZUXIN LI<sup>7</sup>,  
AND YANGMIN LI<sup>8</sup>, (Senior Member, IEEE)

<sup>1</sup>School of Energy and Mechanical Engineering, Jiangxi University of Science and Technology, Nanchang 330013, China

<sup>2</sup>School of Intelligent Systems Science and Engineering, Jinan University, Zhuhai 519070, China

<sup>3</sup>Department of Building and Real Estate, The Hong Kong Polytechnic University, Hong Kong

<sup>4</sup>Guangxi Key Laboratory of Automatic Detecting Technology and Instruments, Guilin University of Electronic Technology, Guilin 541004, China

<sup>5</sup>Artificial Intelligence Key Laboratory of Sichuan Province, Sichuan University of Science and Engineering, Zigong 643000, China

<sup>6</sup>National Engineering Research Center for Advanced Polymer Processing Technology, Zhengzhou University, Zhengzhou 450000, China

<sup>7</sup>School of Engineering, Huzhou University, Huzhou 313000, China

<sup>8</sup>Department of Industrial and Systems Engineering, The Hong Kong Polytechnic University, Hong Kong

Corresponding author: Ping He (pinghecn@qq.com)

This work was supported in part by the National Natural Science Foundation of China under Grant 11705122, Grant 61902268, and Grant 51575544, in part by the Sichuan Science and Technology Program under Grant 2020YFH0124, Grant 2020YJ0368, Grant 2019YFSY0045, Grant 2018GZDZX0046, and Grant 2018JY0197, in part by the Education Department of Jiangxi Province under Grant GJJ170568, in part by the Outstanding Youth Backbone Project of Jinan University under Grant 2019QNGG26, in part by the Hong Kong Research Grants Council under Grant BRE/PolyU 152099/18E and Grant PolyU 15204719/18E, in part by the Natural Science Foundation of The Hong Kong Polytechnic University under Grant G-YW3X, in part by the Guangxi Natural Science Foundation of China under Grant 2018GXNSFAA138092, in part by the Project on Promoting Scientific Research Ability of Young and Middle-aged People in Guangxi under Grant 2018KY1095, in part by the Specialized Talents in Guangxi under Grant AD18281018, in part by the Special Foundation of High-tech Zone of Zigong city under Grant 2021, in part by the Open Foundation of Artificial Intelligence Key Laboratory of Sichuan Province under Grant 2018RZJ01, in part by the Nature Science Foundation of Sichuan University of Science and Engineering under Grant 2017RCL52, in part by the Zigong Science and Technology Program of China under Grant 2019YYJC03 and Grant 2019YYJC15, and in part by the General Research Fund (GRF) under Grant BRE/PolyU 152047/19E and Grant BRE/PolyU15210720.

**ABSTRACT** This paper focuses on improving tracking performance of totally uncoupled compliant micromanipulator based on robust control method of elliptical hysteresis model. The hysteresis model and hysteresis compensation model for proposed mechanism based on Piezoelectric transducer (PZT) are established by using elliptical model method. The values of elliptical hysteresis model parameters are identified by simulating method with different frequencies of control input. The uncertainty model is also established, the values of corresponding estimated parameters are conformed by experiment method. Based on the uncertainty model and elliptical hysteresis model, the robust tracking control method is presented and utilized to evaluate the tracking performance of proposed mechanism under inputting different tracking curves. The proposed method can accurately control the output displacement and improve tracking performance of this mechanism, which are validated and carried out by using experimental studies. Additionally, the coupling errors between two directions are kept within 0.14% and the tracking errors for different curves are within 2.5%.

**INDEX TERMS** Elliptic model, robust control, positioning tracking, micro/nano manipulator.

## I. INTRODUCTION

*Motivation:* With the development of nanotechnology, micro/nano manipulator is more and more paid attention by many scientists. Traditional manufacturing technology has not satisfied the demands of high precision in micromechanical system, but the micro/nano manufacturing technology can meet it. Comparing with traditional

hinge, the flexure hinge owns these advantages of no backlash, no friction, simple structure, and easy manufacture. It has been widely applied in micromanipulator system, such as micro/nano-positioning stage, micro/nano manufacturing, and high-accuracy alignment instrument [1], [2]. Additionally, piezoelectric transducer (PZT) is usually selected as the actuators of compliant micromanipulator system since the advantages of fast response and high precision [3]. Nonetheless, hysteresis phenomenon of PZT and unstable positioning control of compliant mechanism are the main reasons to

The associate editor coordinating the review of this manuscript and approving it for publication was Bin Xu.

restrict further application and development of the PZT-based compliant micromanipulator system [4], [5]. The purpose of this paper is to improve the tracking performance of decoupled precision positioning platform by using elliptic model and robust tracking control methods.

*Brief Summary of Prior Literature:* In past few years, cross coupling characteristic of compliant mechanism is always studied by researchers [6]. A kind of 2-DOFs compliant mechanism with the maximal cross coupling error of  $0.12\mu\text{m}$  under the frequency of 50Hz is developed and designed by [7]. A high-bandwidth 2-DOFs positioning stage with the cross coupling motion of 0.2% at the total workspace of  $15\mu\text{m} \times 15\mu\text{m}$  in two directions is also proposed by [8]. A kind of novel 2-DOFs micromanipulation stage for micro/nano positioning and manipulation is developed by [9], which has the workspace of  $8\mu\text{m} \times 8\mu\text{m}$  with the first natural frequency of 665.4Hz, while the cross-axis coupling error is 2% more than previous results. In addition, a novel 2-DOFs parallel compliant mechanism with the first natural frequency of 763.23Hz has been designed by [10]. From above literatures, it can be known that the coupling error exists in the parallel robot with multi-DOFs, while it can influence the positioning precision of micromanipulator. Therefore, the decoupled performance of compliant mechanism has to be considered and analyzed in this paper.

In the matter of modeling and control for the nonlinear hysteresis effect, researcher has conducted to model and compensate the nonlinear phenomenon caused by PZT [11]. Some modeling techniques of PZT have been also analyzed and presented including the charge steering model, the voltage input electromechanical model, the physical hysteresis model, and the neural network hysteresis model [12]. Other appropriate methods have been also presented based on the established mathematical formulation to approximate the input/output behavior due to hysteresis. For example, the Duhem model, the Maxwell model, and the Preisach model [13], [14]. Otherwise, the nonlinear effect caused by hysteresis phenomenon seriously limits the tracking performance PZT-driven positioning platform. For overcoming this drawback, the hysteresis compensated strategies have been proposed in [15]–[17] to eliminate the errors caused by hysteresis nonlinear. For the position tracking control of the compliant micro motion stage, it is very important in high precision application field. Although the complexity of modeling leads to be hard to control its position due to being lack of accurate computed model, but many control modeling methods are proposed. The loop closure theory, which uses the complex number method to establish the hysteresis model of compliant mechanism, is developed by [18]. This model has been successfully used in the position control of mechanism [19]. A linear scheme method is presented for the displacement analysis of micro positioning stage which linearize the geometric constraint equation of the stage [20]. Based on this method, a new idea of constant Jacobian method for computing the kinematics of mechanism is proposed [21]. Additionally, this method has been also used

in the PID control of a 3-RRR flexure-based mechanism [22]. The positioning control simulation of the compliant mechanism by using sliding mode control has been carried out [23]. Robust adaptive control method is also applied in the four bar micro/nano manipulation [2], [24]. Moreover, a kind of feedback control method for eliminating the hysteresis, non-linearity and drift of PZT has been designed for applying in a 3-DOFs PZT-driven micro positioning stage [25]. Furthermore, some other positioning control methods are presented, such as feed-forward combining with feedback control [26], an adaptive backstepping approach [27], tracking control combining with a feed-forward hysteresis compensation [28], and an observer-based control [29]. In most of above studies, the complex hysteresis inverse model has been adopted to compensate for the hysteresis effect, but it only aims to the piezoelectric actuator while leave out of consideration of the compliant mechanism. The nonlinear behavior and control method are the key factors to obtain the high precision motion of micromanipulator. The existed studies are mostly about the classical hysteresis mode methods. However, for the rate-dependent hysteresis motion of piezoelectric actuator, a elliptical hysteresis model method may be more suitable for establishing the hysteresis model. Additionally, for achieving the stable tracking performance, the robust tracking control is better suitable for control the positioning micromanipulator comparing with the above control methods.

*Contribution of This Paper:* Based on aforementioned discussions, a novel 2-DOFs compliant mechanism with full decoupled is designed, as shown in Figure 1. The robust tracking control method with elliptical hysteresis model is carried out to obtain excellent tracking performance with different desired curves and uncertainty model. The elliptical hysteresis model is also established and its parameters are confirmed by experimental method. With the proposed method, the mechanism shows good positioning tracking

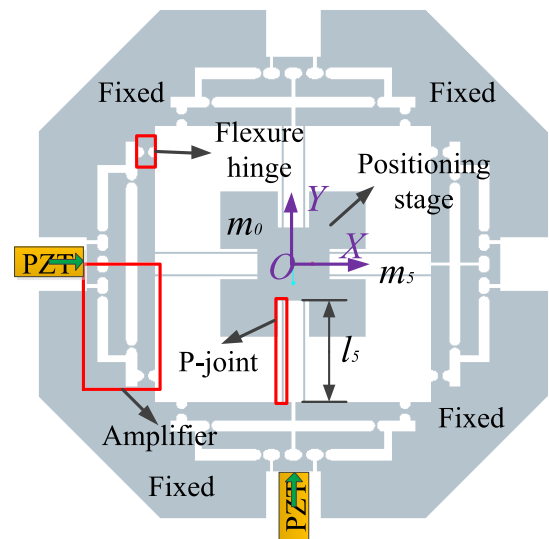


FIGURE 1. Model of decoupled compliant mechanism.

performance in two motion directions. Experimental results indicate that the presented tracking control method can be successfully implemented in micro/nano system. Compared with other works, the novel control method achieves better control result and smaller error.

*The organization of this paper is as follows:* The structure of the PZT-driven fully uncoupled compliant micro/nano-positioning platform is described in Section II. The elliptical hysteresis model, the hysteresis compensation and parameter identification are presented in Section III. The model of uncertainty and the robust motion tracking control methodology are established in Section IV. Experimental studies are detailedly presented and results are listed and discussed in Section V. Finally, the conclusion will be drawn in Section VI.

## II. SYSTEM DESCRIPTION

A kind of novel 2-DOFs micro precision positioning stage has been designed and analyzed in previous work [30], as shown in Figure 1. This stage is composed of a positioning compliant mechanism (PCM) and the piezoelectric transducer (PZT). For this microelectromechanical system, the PCM can be looked as a mass-spring-damper mechanical system and the PZT can be regarded as a force generator that generates force due to the applied voltage [31], [32]. The dynamical equation of this system can be formulated as follows:

$$m\ddot{x} + c\dot{x} + kx = f(u), \quad (1)$$

where  $m$ ,  $c$ , and  $k$  are the mass, damping, and stiffness, respectively,  $f(u)$  ( $= u_{in} - u_h - u_d$ ) is the hysteresis function including input voltage  $u_{in}$ , hysteresis voltage  $u_h$  and external disturbance  $u_d$ ,  $x$  is the output displacement.

## III. HYSTERESIS COMPENSATION AND PARAMETERS IDENTIFICATION

In this section, hysteresis modeling with elliptical equation is established and the values of its corresponding parameters under inputting different frequencies are identified. Additionally, the hysteresis compensation strategy with the inverse hysteresis model principle is also carried out.

### A. HYSTERESIS MODELING

Generally speaking, Hysteresis phenomenon of PZT is known as a rate-dependent hysteresis. In this paper, a novel elliptical modeling method is adopted to represent the rate-dependent hysteresis of PZT. Supposing that the X direction is the input voltage  $U$  and Y direction is the output displacement  $Y$  of the system as shown in Figure 2, the coordinate  $U'O'Y'$  of the elliptical mathematical model is obtained by a rotational angle  $\theta$  and translational motion  $(u_o, y_o)$  along with the world coordinate  $UOY$ .

According to the principle of coordinate transformation, the following equations can be obtained by:

$$\begin{aligned} u_{in} &= u_o + a \cos \theta \cos \alpha - b \sin \theta \sin \alpha, \\ y_{out} &= y_o + a \sin \theta \cos \alpha + b \cos \theta \sin \alpha, \end{aligned} \quad (2)$$

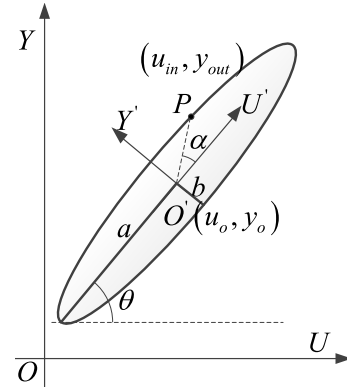


FIGURE 2. Ellipse model description.

where the  $(u_o, y_o)$  is the central point of ellipse,  $a$  and  $b$  are lengths of the major and minor radii, respectively.  $\theta$  is the orientation of the ellipse between the major axis and the X direction.  $\alpha$  is the angle between  $O'P$  and the positive X direction of coordinate plane  $U'O'Y'$ , its value is variable from 0 to  $2\pi$ . Therefore, the equation (2) can be also expressed as the following matrix form:

$$\begin{bmatrix} u_{in} \\ y_{out} \end{bmatrix} = \begin{bmatrix} u_o \\ y_o \end{bmatrix} + \begin{bmatrix} c\theta & -s\theta \\ s\theta & c\theta \end{bmatrix} \begin{bmatrix} a & 0 \\ 0 & b \end{bmatrix} \begin{bmatrix} c\alpha \\ s\alpha \end{bmatrix}. \quad (3)$$

For inputting the different frequency signals, the equation (2) can be rewritten as following:

$$\begin{aligned} u_{in}(t) &= u_o + A \sin(2\pi ft + \beta_1), \\ y_{out}(t) &= y_o + B \sin(2\pi ft + \beta_2), \end{aligned} \quad (4)$$

where  $A = \sqrt{a^2 \sin^2 \theta + b^2 \cos^2 \theta}$ ,  $2\pi ft = \alpha$ ,  $\beta_1 = \arctan [(b/a) \tan \theta]$ ,  $B = \sqrt{a^2 \cos^2 \theta + b^2 \sin^2 \theta}$ ,  $\beta_2 = \arctan [(-b/a) \cot \theta]$ , and  $\beta_1 > \beta_2$ .

*Remark 1:* Based on the elliptical hysteresis model, an expanded input space is constructed to describe the multi values hysteresis function  $H(u)$  by a continuous one-to-one mapping:  $\Re^2 \rightarrow \Re$

### B. RATE-DEPENDENT HYSTERESIS MODELING OF PZT

Figures 3 and 4 are the PZT's output displacements under different frequencies and amplitudes of input voltage, where it can be seen that the results are related with the frequency and amplitude of input signal. Therefore, the hysteresis phenomenon of PZT is the rate-dependent hysteresis phenomenon. Furthermore, the hysteresis loops are also ellipse-like and can be modeled by elliptical equation.

Based on simulated analysis, the parameters of elliptical hysteresis model under different frequencies of input voltage can be identified and their values are listed in Table 1.

### C. HYSTERESIS COMPENSATION STRATEGY

For eliminating the nonlinear influence, an inverse hysteresis model is established in this paper. According to the Remark 1 and equation (4), the discrete hysteresis function

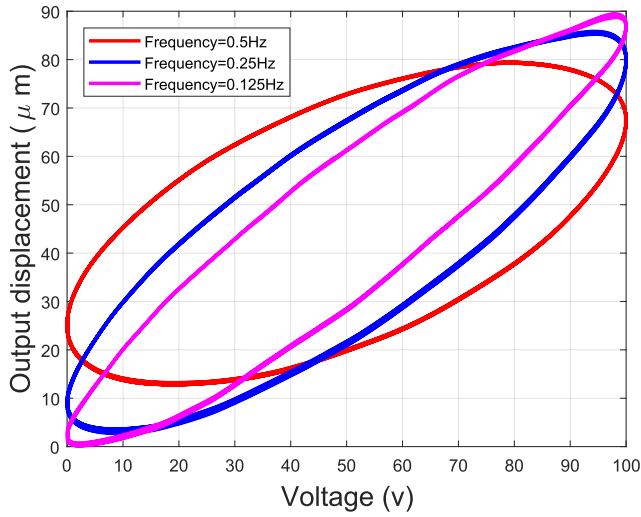


FIGURE 3. The hysteresis loop with input different frequencies.

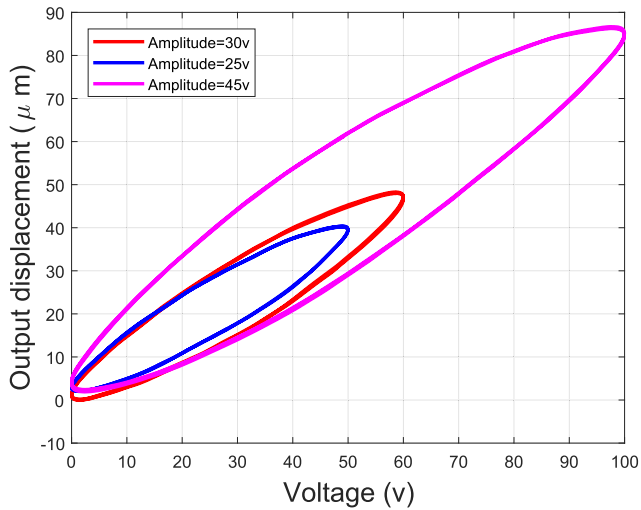


FIGURE 4. The hysteresis loop with input different amplitudes.

TABLE 1. The values of parameters in elliptical model with different frequencies.

| $f(Hz)$ | $x_o(v)$ | $y_o(\mu m)$ | $a(\mu m)$ | $b(\mu m)$ | $\theta(^{\circ})$ |
|---------|----------|--------------|------------|------------|--------------------|
| 0.125   | 49.44    | 44.39        | 64.78      | 12.16      | 42.03              |
| 0.25    | 49.73    | 44.21        | 61.79      | 18.21      | 38.87              |
| 0.5     | 49.75    | 46.15        | 54.90      | 23.87      | 28.17              |

$H(u)$  and the discrete inverse hysteresis model  $H^{-1}(y)$  can be expressed by

$$y(k) = H(u) = Au(k) + Bu(k - 1) + C, \quad (5)$$

where  $A$ ,  $B$ , and  $C$  are respectively the coefficients with respect to frequencies and amplitudes of input voltage.

$$u(k) = H^{-1}(y) = A_1y(k) + B_1y(k - 1) + C_1, \quad (6)$$

where  $A_1$ ,  $B_1$ , and  $C_1$  are the coefficients with respect to frequencies and amplitudes of input reference trajectory, respectively. For a rate-dependent hysteresis model, the feed-

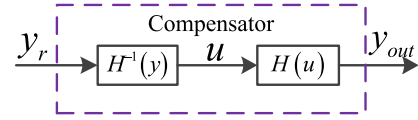


FIGURE 5. The black diagram of hysteresis compensation.

forward controller can be used to compensate the hysteresis nonlinear error, the Figure 5 shows the compensation strategy.

#### IV. UNCERTAINTY ANALYSIS AND ROBUST CONTROLLER DESIGN

##### A. UNCERTAINTIES MODELING

For the system described in equation (1), robust control method can be established for the purpose of high-precision tracking of a specified reference trajectory with the desired command of target performance:

$$u_r = m\ddot{x}_r + c\dot{x}_r + kx_r + u_h + u_d. \quad (7)$$

For achieving the target performance of the system, the output voltage in equation (7) with reference motion trajectory must be equal to input voltage in equation (1). Then the target performance can be established by error equation

$$m_d\ddot{e} + c_d\dot{e} + k_de = 0, \quad (8)$$

where  $e = x - x_r$  is the error from the output displacement to the reference trajectory,  $m_d$ ,  $c_d$ , and  $k_d$  are desired values of the mass, damping, and stiffness of system, respectively.

In practice, the values of parameters in the system (1) are difficult to be determined. However, their estimated values and corresponding bounded values, as well as the bound of the hysteresis effect and external disturbance, are available. Therefore, uncertainty modeling of these parameters in system (1) can be established as following

$$\begin{cases} |\Delta m| = |m - \hat{m}| \leq \delta m, \\ |\Delta c| = |c - \hat{c}| \leq \delta c, \\ |\Delta k| = |k - \hat{k}| \leq \delta k, \\ |u_h + u_d| \leq \delta u_{hd}, \end{cases} \quad (9)$$

where  $\Delta m$ ,  $\Delta c$ , and  $\Delta k$  are the parametric errors,  $\hat{m}$ ,  $\hat{c}$ , and  $\hat{k}$  represent the estimated parameters, and the  $\delta m$ ,  $\delta c$ , and  $\delta k$  denote the bounds of the system parameters and  $\delta u_{hd}$  is the bound of the hysteresis effects and external disturbances. With this assumption, the robust motion tracking control method can be realized.

##### B. ROBUST TRACKING CONTROL METHOD

In this section, the robust control method is applied to solve the problem that the motion tracking control in the PZT-actuated micromanipulation system. Firstly, a special switching function  $s$  is defined as

$$s = \dot{e} + \tau, \quad (10)$$

where the state of a dynamic compensator,  $\tau$ , is used to describe the tracking error, which can be expressed by

$$\dot{\tau} = -\gamma\tau + g_1e + g_2\dot{e}, \quad (11)$$

where  $\gamma$  is a constant scalar and  $\gamma \geq 0$ ,  $g_1$  and  $g_2$  are the control gains related to the target performance equation (8). Differentiating equation (10) with respect to time, it can be obtained

$$\dot{s} = \ddot{e} + \dot{\tau} \quad (12)$$

Substituting equations (11) into (12) with the term  $\tau$  eliminated by using equation (10) to validate the closed-loop dynamics of system under the robust control, the following equation is obtained

$$\ddot{e} + (\gamma + g_2)\dot{e} + g_1e = \dot{s} + \gamma s, \quad (13)$$

Defining the following equations

$$\begin{cases} g_1 = k_d/m_d, \\ g_2 = c_d/m_d - \gamma. \end{cases} \quad (14)$$

The closed-loop system (13) can be rewritten by

$$m_d\ddot{e} + c_d\dot{e} + k_d e = m_d\dot{s} + m_d\gamma s. \quad (15)$$

According to the equation (15), the closed-loop dynamics can achieve to the target performance (8) when the switch function  $s = 0$  and its differential  $\dot{s} = 0$ . Therefore, for letting system to reach the slide mode surface, the control law can be formulated.

*Theorem 1:* For the PZT-driven compliant mechanism system presented by (1) under the uncertainty of parameter and hysteresis effect (9), the system obtains the target performance (8) as the following robust control law

$$u_{rcl} = \hat{m}\ddot{x}_{rq} + \hat{c}\dot{x} + \hat{k}x - \eta s - d \frac{s}{|s|}, \quad (16)$$

where  $\ddot{x}_{rq} = \ddot{x}_r - \dot{\tau}$ ,  $\eta$  is a positive scalar,  $\frac{s}{|s|}$  is a symbolic function and  $\frac{s}{|s|} = \text{sgn}(s)$ , and the term  $d$  is defined by

$$d \geq \delta m |\ddot{x}_{rq}| + \delta c |\dot{x}| + \delta k |x| + \delta u_{hd} + \sigma, \quad (17)$$

where  $\sigma$  is also a positive scalar.

### C. STABILITY ANALYSIS

Defining the following Lyapunov function

$$u(s) = \frac{1}{2}ms^2, \quad (18)$$

which is continuous and non-negative. Differentiating equation (18) with respect to time, it can be got

$$\dot{u}(s) = ms\dot{s}. \quad (19)$$

Otherwise, considering the  $\ddot{x}_{rq} = \ddot{x}_r - \dot{\tau}$ , and  $\ddot{e} = \ddot{x} - \ddot{x}_r$ , the equation (12) can be rewritten by

$$\dot{s} = \ddot{x} - \ddot{x}_{rq}. \quad (20)$$

Substituting equations (20) into (19), the following equation can be obtained as

$$\begin{aligned} \dot{u}(s) &= ms(\ddot{x} - \ddot{x}_{rq}) \\ &= s(u_{in} - c\dot{x} - kx - u_h - u_d - m\ddot{x}_{rq}). \end{aligned} \quad (21)$$

Combining equations (12) and (9) and replacing the term  $u_{in}$  used by control law (16), the following formula is written by:

$$\begin{aligned} \dot{u}(s) &= -\eta s^2 - d|s| + sF \\ &\leq -\eta s^2 - d|s| + |s|F_1, \end{aligned} \quad (22)$$

where  $F = [\Delta m \ddot{x}_{rq} + \Delta c \dot{x} + \Delta k x - (u_h + u_d)]$  and  $F_1 = (\delta m |\ddot{x}_{rq}| + \delta c |\dot{x}| + \delta k |x| + \delta u_{hd})$ .

Substituting equations (20) into (22), which can be repressed by:

$$\dot{u}(s) \leq -\eta s^2 - \sigma |s| \leq 0. \quad (23)$$

The equation (23) shows that  $u(s) \rightarrow 0$  when the switching function  $s \rightarrow 0$  as  $t \rightarrow 0$ . Therefore, the closed-loop system is stable and the motion tracking is converged under the proposed robust tracking control law in the system (1), Theorem 1 and target performance equation (8).

However, during control process, the term  $\text{sgn}(s)$  is a discontinuous function, which will give rise to chatter phenomenon due to the bad switching in the system control. Otherwise, this chattering phenomenon is undesirable when a high-frequency dynamics might be excited. Thus, for eliminating the effect, the concept of boundary layer technology is used to smooth the control input signal. During the switching function  $s \rightarrow 0$ , the discontinuous function  $\text{sgn}(s)$  will be replaced by a saturation function, it can be written by

$$\text{sat}\left(\frac{s}{\Delta}\right) = \begin{cases} -1, & s < -\Delta, \\ \frac{s}{\Delta}, & -\Delta \leq s \leq \Delta, \\ +1, & s > \Delta. \end{cases} \quad (24)$$

where  $\Delta$  is the boundary layer thickness, so the control law (16) can be rewritten by

$$u_{rcl} = \hat{m}\ddot{x}_{rq} + \hat{c}\dot{x} + \hat{k}x - \eta s - d \cdot \text{sat}\left(\frac{s}{\Delta}\right) \quad (25)$$

Based on aforementioned analysis, the accuracy of switching function  $s$  will be guaranteed to stay within the boundary layer. From the closed-loop system (15), the steady-state value  $s_{ss}$  of switching function within the boundary layer can be obtained as

$$s_{ss} = \frac{k_d s_{psse}}{m_d \gamma} \quad (26)$$

where  $s_{psse}$  is the steady-state position error. Considering a standard second-order characteristic equation of the equation (8), the desired parameters can be calculated by

$$m_d = 1, \quad c_d = 2\zeta\omega_n, \quad k_d = \omega_n^2 \quad (27)$$

where  $\zeta$  and  $\omega_n$  are the damping factor and undamped natural frequency.

### D. CONTROL STRATEGY

For the compliant manipulator, the robust tracking motion method with ellipse-based compensator is applied to obtain the control input. The Figure 6 describes the control strategy.

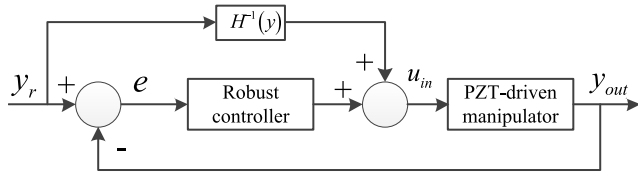


FIGURE 6. The black diagram of robust controller with ellipsoid-based feedforward compensator.

V. EXPERIMENTS

In this section, a series of experiments are carried out. Firstly, the experimental setup is built as shown in Figure 7, and then the lumped parameters of micro/nano-positioning stage are identified by input-output recorded dates, and finally, the open-loop and closed-loop experiments are executed to validate the theory models. All results present that the proposed tracking control method is effective for PZT-driven micromanipulator system.

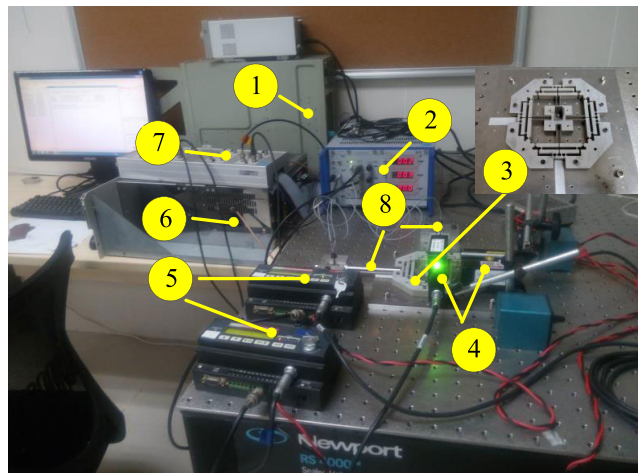


FIGURE 7. The experimental setup. (1) Host computer, (2) Signal amplifier and controller, (3) Compliant mechanism, (4) Laser sensors, (5) Laser collectors, (6) dSPACE controlling system, (7) DAQ board, (8) PZTs.

A. EXPERIMENTAL SETUP

Firstly, the mechanism is fabricated by using Wire-Electrical-Discharge-Machining (WEDM) technique from a piece of material (Al7075-T6). Then experimental setup of the micro-positioning stage is presented as shown in Figure 7. It is composed of a micro/nano-positioning stage, a piezoelectric actuator, an amplifier module, a capacitive position sensor, a signal processing unit, personal computer (PC), and dSPACE real-time simulation system combining a digital-to-analogue (D/A) board and an analog-to-digital (A/D) board. Two PZTs with stroke of 90µm (model P-840.60 produced by Physik Instrumente, Inc.) are adopted to drive the micromanipulator, and the PZTs are driven by a voltage of 0-100V through a three axes piezo-amplifier (E-509 from the PI). Two laser displacement sensors and collectors (Microtrak II, head model: LTC-025-02, from MTI Instrument, Inc.) are used to

measure the end-effector displacements of the two axes. The analog outputs of two sensors are connected to a PCI-based data acquisition (DAQ) board (PCI-6143 with 16-bit A/D converters, from NI Corp.) through a shielded I/O connector block (SCB-68 from NI) with noise rejections. The digital outputs of the DAQ board are read by a PC simultaneously.

B. PARAMETERS CONFIRMED

For the PZT-driven flexure-based micro/nano-positioning platform described in system (1), the robust motion tracking control law (16) is implemented in the dSPACE real-time simulation system. Giving the desired motion trajectory, the tracking ability of the control system can be closely evaluated by experimental method in the presence of parametric uncertainties, non-linearities, and external disturbances. A computational approach can be used to confirm the estimated parameters values of mass, damping, and stiffness. The estimated values of the system parameters and their corresponding bounds are presented in Table 2.

TABLE 2. Lumped parameters of micro/nano-positioning stage.

| Lumped parameter        | Estimated value     | Bound                |
|-------------------------|---------------------|----------------------|
| Mass ( $vs^2/\mu m$ )   | $\hat{m} = 10^{-6}$ | $\delta m = 10^{-6}$ |
| Damping ( $vs/\mu m$ )  | $\hat{c} = 0.00136$ | $\delta m = 0.00136$ |
| Stiffness ( $v/\mu m$ ) | $\hat{k} = 0.46$    | $\delta k = 0.46$    |

According to a rule of thumb, the undamped natural frequency ( $\omega_n$ ) can be estimated by the lowest structural resonance ( $\omega_m$ ), which is confined to  $\omega_n \leq 0.5\omega_m$ .

C. OPEN-LOOP EXPERIMENT

To validate the coupled performance of the proposed mechanism, corresponding experimental tests are firstly carried out. The Figure 8 shows the output displacements and corresponding parasitic motions in X and Y directions when an input voltage ( $u = 25 \sin(\frac{\pi}{4}t - \frac{\pi}{2}) + 25$ ) is applied to PZTs. The results indicate that the actual amplification ratios of the mechanical amplifier in X and Y directions are respectively about 4.32 and 4.34, meanwhile the parasitic motion in the X and Y directions are about 0.28µm and 0.1µm, respectively. Based on the aforementioned analysis, the cross-coupling errors with respect to output displacements are respectively 0.05% and 0.14%, which demonstrates that the proposed compliant mechanism obtains excellent uncoupled performance. The main reasons may come from the assembly error of the system and the preloaded force applied to the PZTs.

D. CLOSED-LOOP EXPERIMENTS

For studying the tracking performance of the proposed compliant mechanism, a desired tracking trajectory with position, velocity, and acceleration, shown in Figure 9, is firstly given out by polynomials of fourth to seventh order with zero

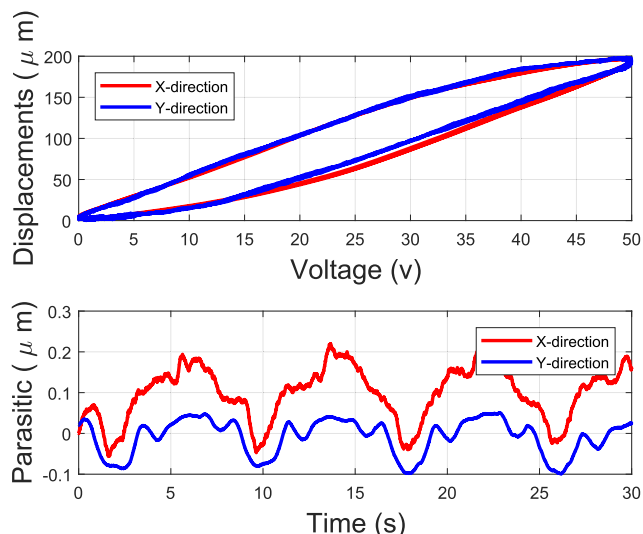


FIGURE 8. The output displacements and parasitic motions in X and Y directions.

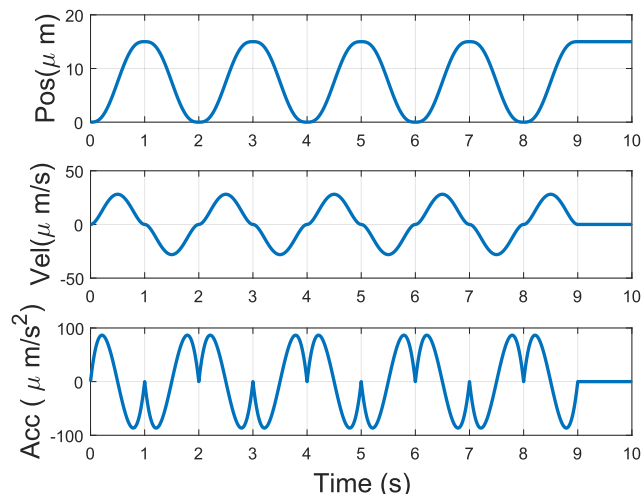
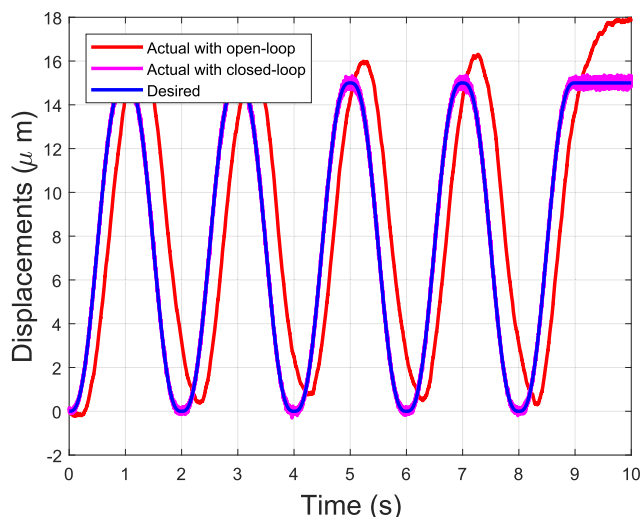


FIGURE 9. The desired trajectory with position, velocity, and acceleration.

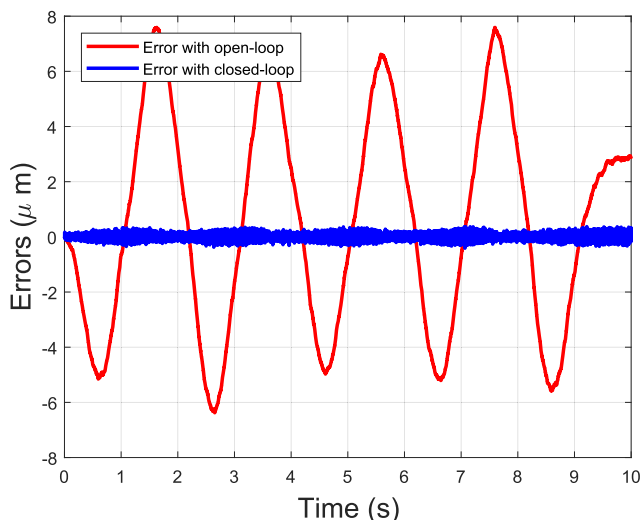
acceleration at the beginning and the end. Then the control method is implemented to evaluate the performance.

**E. TRACKING EXPERIMENTS WITH DIFFERENT TRAJECTORIES**

Due to identical performances in X and Y directions of the compliant mechanism, so the X direction is only selected to carry out the tracking. To the motion trajectory shown in Figure 9, the position tracking and corresponding errors of the micro/nano-positioning platform with open-loop and closed-loop tracking are shown in Figure 10, it can be seen that the closed-loop control obtains the excellent tracking performance comparing with the open-loop control. Otherwise, control law and switching function  $s$  are shown in Figure 11. The switching function expresses that the system can move well within the boundary layer thickness  $\Delta = 2.9mm/s$  specified in (24), which indicates that the closed-loop system



(a) Tracking motions with open-loop and closed-loop control.



(b) The corresponding errors.

FIGURE 10. Tracking control.

excellently traces the desired trajectory closely with the switching function kept to a minimum. The tracking errors indicate that the robust control law can be successfully suitable for the closed-loop system. The experimental results show that the position tracking error is less than 2.5% during dynamic motion.

For further validating the tracking performance of micro/nano-positioning platform, the signal with different frequencies is also applied as the reference input displacement, the Figure 12 shows the tracking result and corresponding error. The result demonstrates that the input displacement is well tracked by the output displacement and the error is less than 0.04%. That's to say the robust control method can effectively eliminate the nonlinear effect caused by rate-dependent of the PZT.

Otherwise, the triangular wave is also carried out to further illustrate the tracking performance of the micromanipulator

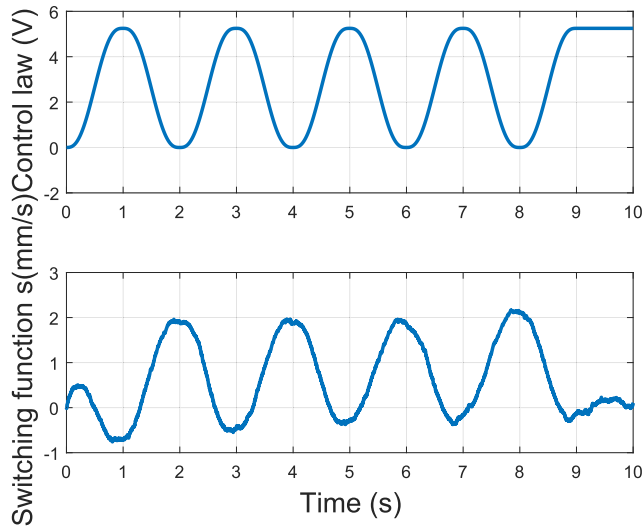


FIGURE 11. The control law and switching function.

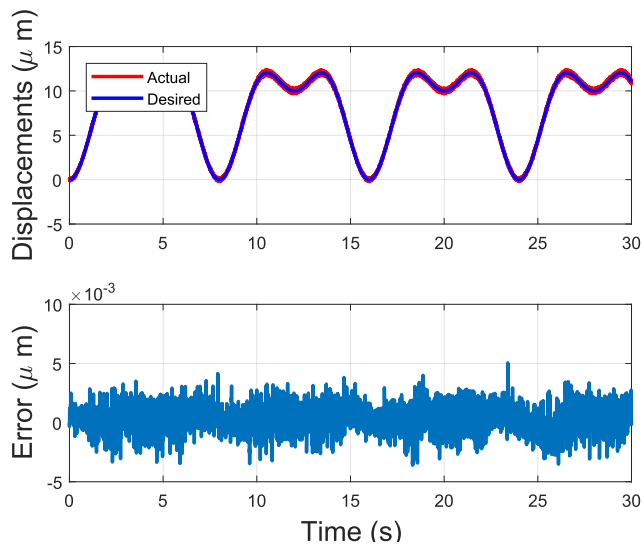


FIGURE 12. The tracking result and error of the signal with different frequencies.

system. As shown in Figure 13, the tracking results indicate that the output wave traces excellently the desired triangular wave and the tracking error is less than 0.02%.

**F. THE 2-DOFs TRACKING TEST**

Based on the aforementioned experiments, the 1-DOF motion tracking is well verified through using the different input signals. The circle trajectory signal with 2-DOFs is used as the reference input. The tracking result and the corresponding error are presented in Figure 14, which indicates that the maximal errors in X and Y directions are at the starting point, respectively.

**G. DISCUSSIONS**

Based on aforementioned analysis, modeling, and experiments, all results demonstrate that the proposed 2-DOFs

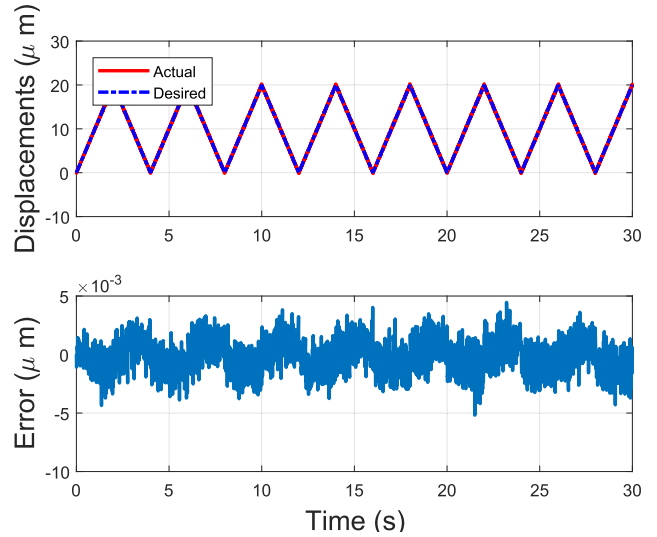


FIGURE 13. The tracking result and error of the triangular wave.

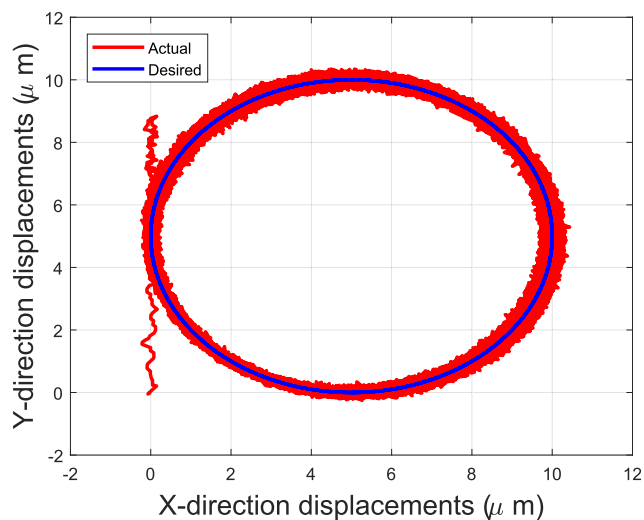
micro/nano-positioning platform owns these advantages of large motion, low cross coupling, and excellent tracking characteristic. Otherwise, robust control can effectively eliminate the phenomenon of rate-dependent hysteresis and has good robustness and stability. A comparison with other proposed nano-positioning stage is presented in Table 3. The natural frequencies of the stages in Refs. [3] and [12] are higher than other studies, but their working ranges are smaller, which seriously limit their further application. Additionally, the performance in terms of cross coupling and workspace of the other two stages in Refs. [6], [8] and [13] are obviously lower than the proposed in this paper. Therefore, in summary, our proposed compliant mechanism possesses the significant advantage in the micromanipulation field. Additionally, the ratio of the coupling to the workspace (RCW) can reflect the decoupled property of micromanipulator. That's to say the smaller the ratio is, the better the performance is. From the Table 3, it can be seen that this study obtains the smallest RCW (0.07%) than other studies, so the proposed mechanism can meet the requirement of performance.

TABLE 3. Property comparisons for proposed similar stages.

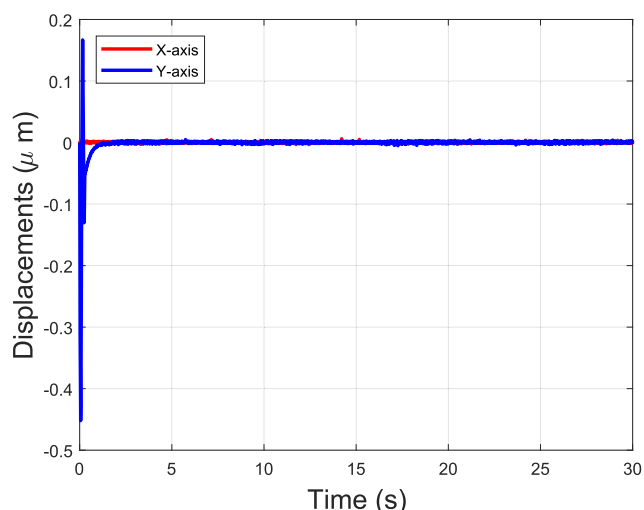
| Ref.      | Frequency (Hz) | Coupling (%) | Workspace ( $\mu m^2$ ) | RCW % |
|-----------|----------------|--------------|-------------------------|-------|
| [3]       | 2.7k           | /            | 25 × 25                 | /     |
| [6]       | 831            | 2            | 119.7 × 121.4           | 1.64  |
| [8]       | 720.52         | 5            | 19.2 × 18.8             | 26.04 |
| [12]      | 2k             | 0.2          | 15 × 15                 | 1.33  |
| [13]      | 665.4          | 2            | 8 × 8                   | 25    |
| Section V | 354.21         | 0.14         | 194.5 × 195.5           | 0.07  |

Moreover, from the control results of robust tracking control method, it can be seen that the closed-loop control owns better position tracking performance than the open-loop control, which indicates that the proposed control method can





(a) The circle tracking



(b) The corresponding error

**FIGURE 14.** 2-DOFs tracking.

verify the theoretical models and the hysteresis compensator is valid. Otherwise, the platform has also excellently effect of displacement tracking for multi-frequency desired value and triangular wave. For further analyzing the stability of stage, multi-input and multi-output displacements are carried out as shown in Figure 14, it can be seen that the desired displacement with two directions input is effectively tracked, while steady-state error is very small.

## VI. CONCLUSION

In this paper, the robust tracking control method with the compensator was proposed and applied for evaluating the tracking performance of the 2-DOFs compliant mechanism. The tracking error could be effectively reduced by elliptical hysteresis model and hysteresis compensator, the model parameters were also identified. The open-loop experimental results expressed that maximal cross coupling error was

0.14% under the workspace for  $194.5\mu\text{m} \times 195.5\mu\text{m}$  with the natural frequency of 354.21Hz. Then closed-loop tracking control experimental results indicated that tracking error for input signal with sine function was up to 2.5%. However, the desired displacements with different trajectories were well tracked by the output displacement and their errors were all less than 0.04%. Additionally, for the multi-input and multi-output tracking control, the result also represented that the system obtained excellent tracking capacity. In future work, other intelligent controllers will be implemented to control the micro/nano-positioning stage and applied in the micro assembly and micro/nano manufacturing field.

## REFERENCES

- [1] Y. Tian, B. Shirinzadeh, and D. Zhang, "A flexure-based mechanism and control methodology for ultra-precision turning operation," *Precis. Eng.*, vol. 33, no. 2, pp. 160–166, Apr. 2009.
- [2] H. C. Liaw, B. Shirinzadeh, and J. Smith, "Robust motion tracking control of piezo-driven flexure-based four-bar mechanism for micro/nano manipulation," *Mechatronics*, vol. 18, no. 2, pp. 111–120, Mar. 2008.
- [3] Y. Kuan Yong, S. S. Aphale, and S. O. Reza Moheimani, "Design, identification, and control of a flexure-based XY stage for fast nanoscale positioning," *IEEE Trans. Nanotechnol.*, vol. 8, no. 1, pp. 46–54, Jan. 2009.
- [4] Y.-Q. Yu, Z.-C. Du, J.-X. Yang, and Y. Li, "An experimental study on the dynamics of a 3-RRR flexible parallel robot," *IEEE Trans. Robot.*, vol. 27, no. 5, pp. 992–997, Oct. 2011.
- [5] Q. Yao, J. Dong, and P. M. Ferreira, "Design, analysis, fabrication and testing of a parallel-kinematic micropositioning XY stage," *Int. J. Mach. Tools Manuf.*, vol. 47, no. 6, pp. 946–961, May 2007.
- [6] J. Dong, D. Mukhopadhyay, and P. M. Ferreira, "Design, fabrication and testing of a silicon-on-insulator (SOI) MEMS parallel kinematics XY stage," *J. Micromech. Microeng.*, vol. 17, no. 6, pp. 1154–1162, 2007.
- [7] C. J. Lin and P. T. Lin, "Particle swarm optimization based feedforward controller for a XY PZT positioning stage," *Mechatronics*, vol. 22, no. 5, pp. 614–628, 2012.
- [8] S. Polit and J. Dong, "Development of a high-bandwidth XY nanopositioning stage for high-rate micro-/nanomanufacturing," *IEEE/ASME Trans. Mechatronics*, vol. 16, no. 4, pp. 724–733, Aug. 2011.
- [9] Y. Qin, B. Shirinzadeh, Y. Tian, and D. Zhang, "Design issues in a decoupled XY stage: Static and dynamics modeling, hysteresis compensation, and tracking control," *Sens. Actuators A, Phys.*, vol. 194, pp. 95–105, May 2013.
- [10] P. Liu, P. Yan, Z. Zhang, and T. Leng, "Modeling and control of a novel X–Y parallel piezoelectric-actuator driven nanopositioner," *ISA Trans.*, vol. 56, pp. 145–154, May 2015.
- [11] G. Zhang, P. He, H. Li, H. Liu, X.-Z. Xiong, Z. Wei, W. Wei, and Y. Li, "An incremental feedback control for uncertain mechanical system," *IEEE Access*, vol. 8, no. 1, pp. 20108–20117, 2020.
- [12] X. Dang and Y. Tan, "An inner product-based dynamic neural network hysteresis model for piezoceramic actuators," *Sens. Actuators A, Phys.*, vol. 121, no. 2, pp. 535–542, Jun. 2005.
- [13] H. Tang and Y. Li, "Design, analysis, and test of a novel 2-DOF nanopositioning system driven by dual mode," *IEEE Trans. Robot.*, vol. 29, no. 3, pp. 650–662, Jun. 2013.
- [14] H. C. Liaw and B. Shirinzadeh, "Neural network motion tracking control of piezo-actuated flexure-based mechanisms for micro-/Nanomanipulation," *IEEE/ASME Trans. Mechatronics*, vol. 14, no. 5, pp. 517–527, Oct. 2009.
- [15] R. B. Mrad and H. Hu, "A model for voltage-to-displacement dynamics in piezoceramic actuators subject to dynamic-voltage excitations," *IEEE/ASME Trans. Mechatronics*, vol. 7, no. 4, pp. 479–489, Dec. 2002.
- [16] Z. Tong, Y. Tan, and X. Zeng, "Modeling hysteresis using hybrid method of continuous transformation and neural networks," *Sens. Actuators A, Phys.*, vol. 119, no. 1, pp. 254–262, Mar. 2005.
- [17] W. T. Ang, P. K. Khosla, and C. N. Riviere, "Feedforward controller with inverse rate-dependent model for piezoelectric actuators in trajectory-tracking applications," *IEEE/ASME Trans. Mechatronics*, vol. 12, no. 2, pp. 134–142, Apr. 2007.

- [18] L. L. Howell and A. Midha, "A loop-closure theory for the analysis and synthesis of compliant mechanisms," *J. Mech. Des.*, vol. 118, no. 1, pp. 121–125, Mar. 1996.
- [19] T.-F. Lu, D. C. Handley, and Y. K. Yong, "Position control of a 3-DOF compliant micro-motion stage," in *Proc. Control, Autom., Robot. Vis. Conf.*, 2004, vol. 2, no. 5, pp. 1274–1278.
- [20] I. Her and J. C. Chang, "A linear scheme for the displacement analysis of micropositioning stages with flexure hinges," *J. Mech. Des.*, vol. 116, no. 3, pp. 770–776, Sep. 1994.
- [21] W. J. Zhang, J. Zou, L. G. Watson, W. Zhao, G. H. Zong, and S. S. Bi, "The constant-Jacobian method for kinematics of a three-DOF planar micro-motion stage," *J. Robot. Syst.*, vol. 19, no. 2, pp. 63–72, Feb. 2002.
- [22] T.-F. Lu, D. C. Handley, Y. K. Yong, and E. Craig, "A three-DOF compliant micromotionstage with flexure hinges," *Ind. Robot, Int. J.*, vol. 31, no. 4, pp. 355–365, 2004.
- [23] K. Fite and M. Goldfarb, "Position control of a compliant mechanism based micromanipulator," in *Proc. IEEE Int. Conf. Robot. Autom.*, vol. 3, May 1999, pp. 2122–2127.
- [24] H. Shieh and P. Huang, "Adaptive tracking control of a piezoelectric micropositioner," in *Proc. 1st IEEE Conf. Ind. Electron. Appl.*, May 2006, pp. 1–5.
- [25] S. C. Chang, C. K. Tseng, and H. Chien, "An ultraprecision XYθz piezo-micropositioner," *IEEE Trans. Ultrason., Ferroelectr., Freq. Control*, vol. 46, no. 4, pp. 906–912, Jul. 1999.
- [26] Y. Li, Z. Wu, and X. Zhao, "Optimal design and control strategy of a novel 2-DOF micromanipulator," *Int. J. Adv. Robot. Syst.*, vol. 10, no. 3, p. 162, Mar. 2013.
- [27] Y. Li and Z. Wu, "Design, analysis and simulation of a novel 3-DOF translational micromanipulator based on the PRB model," *Mech. Mach. Theory*, vol. 100, pp. 235–258, Jun. 2016.
- [28] H. Tang and Y. Li, "A new flexure-based Yθ nanomanipulator with nanometer-scale resolution and millimeter-scale workspace," *IEEE/ASME Trans. Mechatronics*, vol. 20, no. 3, pp. 1320–1330, Jun. 2015.
- [29] S. Tong, L. Zhang, and Y. Li, "Observed-based adaptive fuzzy decentralized tracking control for switched uncertain nonlinear large-scale systems with dead zones," *IEEE Trans. Syst., Man, Cybern., Syst.*, vol. 46, no. 1, pp. 37–47, Jan. 2016.
- [30] Z. Wu, Y. Li, and M. Hu, "Design and optimization of full decoupled micro/nano-positioning stage based on mathematical calculation," *Mech. Sci.*, vol. 9, no. 2, pp. 417–429, Nov. 2018.
- [31] S. B. Choi, S. S. Han, Y. M. Han, and B. S. Thompson, "A magnification device for precision mechanisms featuring piezoactuators and flexure hinges: Design and experimental validation," *Mechanism Mach. Theory*, vol. 42, no. 9, pp. 1184–1198, Sep. 2007.
- [32] U. Bhagat, B. Shirinzadeh, L. Clark, Y. Qin, Y. Tian, and D. Zhang, "Experimental investigation of robust motion tracking control for a 2-DOF flexure-based mechanism," *IEEE/ASME Trans. Mechatronics*, vol. 19, no. 6, pp. 1737–1745, Dec. 2014.



**ZHIGANG WU** received the B.S. degree from the North University of China, in July 2010, the M.S. degree in mechanical engineering from the Tianjin University of Technology, in March 2013, and the Ph.D. degree from the University of Macau, in June 2017.

He is currently an Associate Professor with the School of Energy and Machinery Engineering, Jiangxi University of Science and Technology, Nanchang, China. His current research interests include precision drive system and micro/nano positioning systems, intelligent optimization algorithms, micro-robot, robotic advanced control algorithm, smart sensors, and bio-robotic systems.



**MIN CHEN** received the B.S. degree from the Jiangxi University of Science and Technology, Nanchang, China, in July 1995, and the M.S. degree in mechanical engineering from Nanchang University, in June 2002.

He is currently an Associate Professor with the School of Energy and Machinery Engineering, Jiangxi University of Science and Technology. His current research interests include mobile robots, robot control, route planning algorithm, mechanism design, intelligent optimization algorithms, smart sensors, video/image tracking algorithm, and UVA.



**PING HE** was born in Huilongya, Nanchong, China, in November 1990. He received the B.S. degree in automation from the Sichuan University of Science and Engineering, Zigong, Sichuan, China, in June 2012, the M.S. degree in control science and engineering from Northeastern University, Shenyang, Liaoning, China, in July 2014, and the Ph.D. degree in electromechanical engineering from the Universidade de Macau, Taipa, Macau, in June 2017.

From December 2015 to November 2018, he was an Adjunct Associate Professor with the Department of Automation, Sichuan University of Science and Engineering. From August 2017 to August 2019, he was a Postdoctoral Research Fellow with the Emerging Technologies Institute, The University of Hong Kong, and the Smart Construction Laboratory, The Hong Kong Polytechnic University. Since December 2018, he has been a Full Professor with the School of Intelligent Systems Science and Engineering, Jinan University, Zhuhai, Guangdong, China. He has authored two books and more than 50 articles. His research interests include robot, sensor networks, complex networks, multiagent systems, artificial intelligence, control theory, and control engineering.

Dr. He is the Reviewer Member of the Mathematical Reviews of American Mathematical Society. He was a recipient of the Liaoning Province of China Master's Thesis Award for Excellence, in March 2015, and the IEEE Robotics and Automation Society Finalist of Best Paper Award, in July 2018. He also serves as a Section Editor of *Automatika: Journal for Control, Measurement, Electronics, Computing and Communications*, an Academic Editor of *PLOS ONE*, and an Associate Editor of *Proceedings of the Institution of Mechanical Engineers, Part E: Journal of Process Mechanical Engineering* and the *IET The Journal of Engineering*.



**HENG LI** was born in Hunan, China, in 1963. He received the B.S. and M.S. degrees in civil engineering from Tongji University, in 1984 and 1987, respectively, and the Ph.D. degree in architectural science from The University of Sydney, Australia, in 1993.

From 1993 to 1995, he was a Lecturer with James Cook University. From 1996 to 1997, he was a Senior Lecturer with the Civil Engineering Department, Monash University. Since 1997, he has been gradually promoted from an Associate Professor to a Chair Professor of construction informatics with The Hong Kong Polytechnic University. He has authored two books and more than 500 articles. His research interests include building information modeling, robotics, functional materials, and the Internet of Things.

Dr. Li was a recipient of the National Award from the Chinese Ministry of Education, in 2015, and the Gold Prize of Geneva Innovation, in 2019. He is a Reviews Editor of *Automation in Construction*. He is also an Editorial Board Member of *Advanced Engineering Informatics*.



**QI ZHANG** (Member, IEEE) received the B.S. and M.S. degrees from the School of Mechanical Engineering, Nanjing University of Science and Technology, Nanjing, China, in 2002 and 2004, respectively, and the Ph.D. degree from the School of Electronic Information and Electrical Engineering, Shanghai Jiaotong University, Shanghai, China, in 2008.

He is currently an Associate Professor with the School of Electronic Engineering and Automation, Guilin University of Electronic Technology, Guilin, China. His research interests include computer vision and microrobot control.



**XINGZHONG XIONG** received the B.S. degree in communication engineering from the Sichuan University of Science and Engineering, Zigong, China, in 1996, and the M.S. and Ph.D. degrees in communication and information system from the University of Electronic Science and Technology of China (UESTC), in 2006 and 2009, respectively. In 2012, he completed a Research Assignment with the Postdoctoral Station of Electronic Science and Technology, UESTC. He is currently a Professor with the School of Automation and Information Engineering, Sichuan University of Science and Engineering. His research interests include wireless and mobile communications technologies, intelligent signal processing, the Internet-of-Things technologies, and very large-scale integration (VLSI) designs.



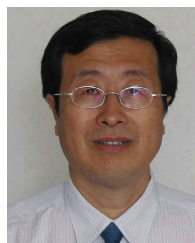
**HAO-YANG MI** received the bachelor's and Ph.D. degrees from the Faculty of Mechanical Engineering, South China University of Technology, Guangzhou, China, in 2010 and 2015, respectively.

From 2016 to 2018, he was a Postdoctoral Researcher with the University of Wisconsin Madison, USA. From 2018 to 2019, he was a Research Fellow with The Hong Kong Polytechnic University. He is currently an Associate Professor with the National Engineering Research Center for Advanced Polymer Processing Technology, Zhengzhou University. He also directs several projects on artificial intelligence and flexible sensors. He has published nearly 100 SCI journal publications so far, with a total citation more than 2000 and an H-index of 27. He has composed a book chapter. He has applied 17 U.S. and China patents. He serves as a regular reviewer for many journals. His current research interests include intelligent materials, artificial intelligence, detection technology, automation device, and flexible sensors.



**ZUXIN LI** was born in Zhejiang, China, in 1972. He received the B.S. degree in industrial automation from the Zhejiang University of Technology, China, in 1995, the M.S. degree in communication and information system from Yunnan University, China, in 2002, and the Ph.D. degree in control theory and control engineering from the Zhejiang University of Technology, in 2008.

From May 2009 to March 2013, he was a Post-doctoral Research Fellow with the Institute of Cyber-Systems and Control, Zhejiang University, China. From August to November 2013, he was a Visiting Scholar with Dalhousie University, Canada. He is currently a Full Professor with the School of Engineering, Huzhou University, China. His research interests include networked control systems, robust control, estimation, prognostics, and health management.



**YANGMIN LI** (Senior Member, IEEE) received the B.S. and M.S. degrees in mechanical engineering from Jilin University, Changchun, China, in 1985 and 1988, respectively, and the Ph.D. degree in mechanical engineering from Tianjin University, Tianjin, China, in 1994.

He started his academic career, in 1994. He was a Lecturer with the Mechatronics Department, South China University of Technology, Guangzhou, China. From May to November 1996, he was a Fellow with the International Institute for Software Technology, United Nations University (UNU/IIST). He was a Visiting Scholar with the University of Cincinnati, in 1996. He was a Postdoctoral Research Associate with Purdue University, West Lafayette, IN, USA, in 1997. He was an Assistant Professor, from 1997 to 2001, an Associate Professor, from 2001 to 2007, and a Full Professor, from 2007 to 2016, all with the University of Macau. He is currently a Full Professor with the Department of Industrial and Systems Engineering, The Hong Kong Polytechnic University, Hong Kong. He has authored or coauthored more than 400 scientific articles in journals and conferences. His research interests include micro/nanomanipulation, compliant mechanism, precision engineering, robotics, and multibody dynamics and control.

Dr. Li is an Associate Editor of the IEEE TRANSACTIONS ON AUTOMATION SCIENCE AND ENGINEERING, *Mechatronics*, IEEE ACCESS, and the *International Journal of Control, Automation, and Systems*.

...